



## Responses of the topside ion fractions concentration over the Arecibo Observatory to solar and geomagnetic activity for the summer period.

Christiano Garnett Marques Brum<sup>(1)</sup>, Nestor Aponte<sup>(1)</sup>, Angela M. Santos<sup>(2)</sup>, and Michael Sulzer<sup>(1)</sup>

(1) Arecibo Observatory, University of Central Florida (UCF), Puerto Rico.

(2) National Institute for Space Research (INPE), Brazil.

### Abstract

In this work, we are analyzing incoherent scatter radar (ISR) data for  $H^+$ ,  $He^+$ , and  $O^+$  ion fractions from the Arecibo Observatory for the period of June solstice (May, June, July, and August) for 1998 and 2000 with respect to solar flux and geomagnetic variations. Due to the strait dependence of the response of the ion fractions with the mentioned forcing, we isolated the real contribution of these parameters by local time and altitude as variation rates. Our results demonstrate that within the altitude range of this work (350 to 1250km) a positive (negative) response of the ion  $O^+$  ( $H^+$ ) with the variation of solar flux while the dependence of  $He^+$  rates presented three different behaviors dependents of time and altitude. Additionally, we found evidence of a small layer formation of  $He^+$  soon after the local midnight in altitudes around 875km with increased geomagnetic activity. A strong dependence with the variation of geomagnetic activity was detected for the ions of  $H^+$  and  $O^+$  post-midnight, which generated two layers. However, these layers were located in different altitudes, far from each other for about 340km.

### 1 Introduction

The topside ionosphere lies above the  $F_2$  peak and merges into the protonosphere where  $H^+$  ions dominate. The ion–electron plasma assumes a distribution close to that appropriated to diffuse equilibrium under gravity (atomic and molecular mass diffusion), with departures from diffusive equilibrium arising from the effect of such factors as neutral winds and electric fields (MacPherson, 1997). The major constituents in the topside ionosphere are  $H^+$ ,  $O^+$  and  $He^+$ . At higher altitudes, the high masses of the molecular species cause their concentrations to decrease to a level where they are no longer available for reaction with  $O^+$ , and thus the resonant charge exchange reaction with hydrogen becomes the main conversion process (Gonzalez, 1994). Since photoionization of the neutral H is negligible because of the low hydrogen concentration in the thermosphere, this is a major source of the  $H^+$  in this region (Gonzalez, 1994).

In this work we are comparing incoherent scatter radar data of the  $H^+$ ,  $He^+$  and  $O^+$  fractions for the summer months (May, June, July and August) from two years (1998 and 2000) with solar flux and geomagnetic variations. These data cover a significant variation of the solar activity (here

quantified by the decimetric solar fluxes value – F10.7cm) of almost 94 SFU (1 SFU =  $10^{-22}W/(m^2Hz)$ ), with a major value of the 190.3 SFU. In fact, the major value of F10.7cm flux was chosen based on in previous results that shown that there is a limit of saturation of the linear dependence of the ions fractions for values around up to 200 SFU. The range of variation with respect to geomagnetic activity is around 2 units of the  $k_p$  index, representing quiet, moderate and disturbed geomagnetic activity, following the criteria of Wrenn et al. (1987). Table 1 summarizes the geophysical conditions of the periods in study.

**Table 1.** Daily F10.7cm solar Flux levels along with Mean  $k_p$  index for the nights analyzed.

	26 May 1998	27 May 1998	23 June 1998	19 August 1998	1 July 2000	6 July 2000
F10.7cm	96.6	101.1	107.5	141.9	168.0	190.3
$k_p$	~1.53	~1.53	~3.12	~3.11	~2.30	~1.38

### 2 Methodology

Due to the reduced number of available days for this study (summer period) and the strait dependence of the response of ion fractions with the solar and geomagnetic variations, we decided to isolate the real contribution of these parameters. For this, we are computing the contribution of the solar flux and geomagnetic activity for each ion fraction. We chose the linear regression method (LR) to obtain the behavior of the ion fractions in study with the solar activity and geomagnetic variations (following the criteria used by Brum et al., 2011). This method is based on regression analysis in which observational data are modeled by a function which is a linear combination of the model parameters and depends on one or more independent variables. For our purpose, we are estimating separately the best “linear fit” of the data with the variables in study and, this way to obtain the individual contribution of these variables in the total sum of ion fraction, with the assumption that  $[H^+]+[He^+]+[O^+]=1$ . So, the fraction of determinate ion ( $I_{(k_p,F10.7,h,t)}$ ) dependent of  $k_p$ , F10.7, altitude ( $h$ ) and local time ( $t$ ) can be obtained by:

$$I_{(k_p,F10.7,h,t)} = Ia_{k_p}(h, t) + kp.Ib_{k_p}(h, t) + Ia_{F10.7}(h, t) + F10.7.Ib_{F10.7}(h, t) + \varepsilon(h, t) \quad (1)$$

Where  $Ia_{kp}(h,t)$  and  $Ia_{F10.7}(h,t)$  are the values of the ions  $I$  for the condition of  $kp=0$  and  $F10.7=0$ , respectively (these terms are not found in nature, they have just mathematical meaning), and  $Ib_{kp}(h,t)$ ,  $Ib_{F10.7}(h,t)$  are the ion fraction rates of electron for the variation of  $kp$  and  $F10.7$  for the ion  $I$ .  $\varepsilon(h,t)$  is the observational error, i.e., the difference between the data and the value obtained by the compute of the linear regression dependent of the chose variables. As example of the methodology described above, Figure 1 shows two blocks of panels representing the extraction of the dependence of the  $H^+$  fraction in function of  $F10.7$ cm (upper block of panels) and  $kp$  index (bottom of block panels). The scatter plots show the linear dependence of the  $H^+$  ion to the geophysical conditions. The bottom panel show the coefficients obtained from the LR interactions above and the vertical bars represents the average between the difference of the data and the values obtained by the linear regression method. The altitudinal of the ion rates were obtained by polynomial approximation (see Garzón et al., 2011; Goncharenko et al., 2013).

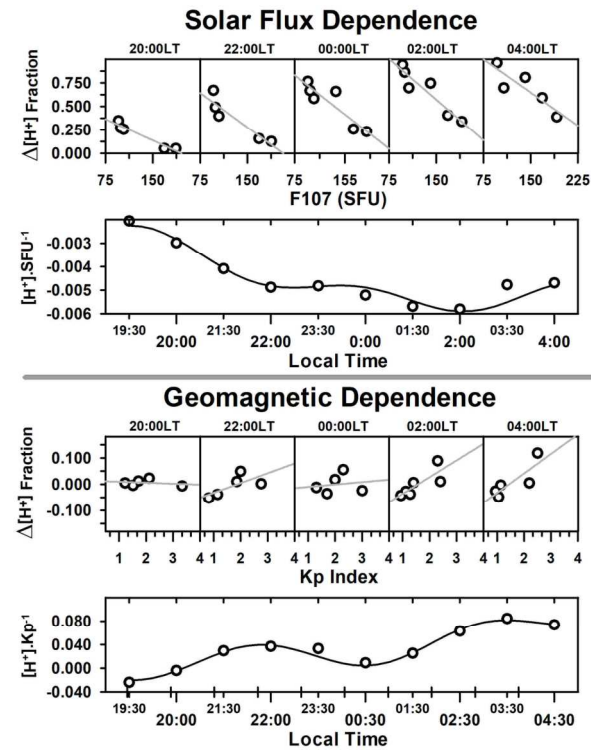


**Figure 1.** Example of the how the LR coefficients were taken. The scatter plot of each block of panels are showing the  $H^+$  fraction by the solar flux and  $kp$  index variation (upper and bottom block, respectively), while the bottom panels are showing the rates  $H^+b_{F10.7}(h,t)$  and  $H^+b_{kp}(h,t)$  (left and right panels, respectively) by local time. This example is for the altitude of 1000km.

### 3 Results

Here we present the climatology of the ion fractions over Arecibo. The variability of the rates in time and altitude for the summer season to solar and geomagnetic activity are addressed below.

### 3.1 Solar activity control of topside-protonosphere ion fraction

The ions fraction rate dependence by the solar flux are showed in the bottom panels of Figure 2. The isoline panels present the ions fraction rate contour plots by local time and altitude while the bottom panels present the vertical cuts of the same parameters for five different times for the ion fractions of  $H^+$ ,  $O^+$  and  $He^+$  (panels a, b and c, respectively). The rates profiles are showing positive (negative) responses of the ion  $O^+$  ( $H^+$ ) ion fraction rate with the increase (decrease) of solar flux during nighttime (panels a and b). In fact, under solar maximum conditions, high temperatures and low neutral atomic hydrogen concentrations results in a decrease of the  $H^+$  fraction and consequently an increase of  $O^+$  fraction in the total amount of Ne (Gonzales, 1994). Otherwise, at the solar minimum there is an abundance of the neutral hydrogen and a lowering of the exospheric scale height (Macpherson, 1997). The decrease of the scale height and the increase of atomic H lead to higher  $H^+$  densities through the very known strong charge exchange chemical reaction between  $O^+$  and  $H^+$  (the resonant charge exchange reaction). The  $He^+$  fraction rate presented three different behaviors in altitude dependents of time, i.e., it was detected two regions of behavior inversion, one in altitudes around  $\sim 513$ km and other one  $\sim 932$ km (positive-to-negative and vice-versa, respectively) at 00:00 LT and with a minimum value at  $\sim 797$ km at 04:00LT (Figure 2, panel c). The losses dependence layer with solar flux of  $He^+$  fraction (region included between the dense black lines of the panel c) is representing the response of the production-loss helium ion processes dependent of the neutral concentration, i.e., under the studied conditions, the contribution of transport in this layer can be neglected. Above the higher transition of  $He^+$  rate (positive negative to positive dependence with  $f10,7$ cm) we found evidences of the formation of the  $He^+$  layer with the increase of the solar activity due to the enhancement of the perpendicular-northward drifts.

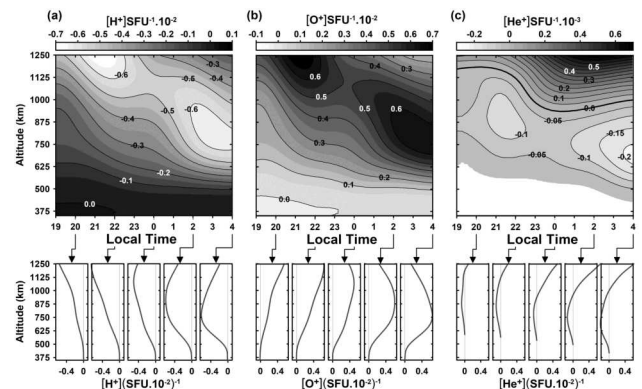


**Figure 2.** Ion fraction dependence with solar activity. Panels a, b and c are showing the ions fraction rates contour plots by local time and altitude with interval of  $5 \cdot 10^{-4}$  ( $H^+$  and  $O^+$ ) and  $5 \cdot 10^{-5}$  ( $He^+$ )  $[I](SFU)^{-1}$ . The profile panels are showing the vertical cuts of the ions fraction rates for five different hours.

### 3.2 Geomagnetic activity control of topside-protonosphere ion fraction

The ions fraction dependence by the geomagnetic activity is showed in Figure 3 with the same disposition presented in the Figure2. Before the local midnight it was not found significant changes in the ion fractions rates below 895 km of altitude. However, above this altitude at the same period we noticed a little increase of the  $H^+$  rate proportional to the sum of decrease of the  $He^+$  and  $O^+$  rates. Soon after midnight the  $O^+$  rate decreases and its losses peak goes downs very fast, passing from altitudes above to 1250km to 900km in less than 4 hours with a minimum rate of the  $\sim 115 \cdot 10^{-3} [O^+].kp^{-1}$  at 04:00LT. During this time the  $He^+$  and  $H^+$  rates increase very fast. The  $H^+$  rate production peak follows almost the same path of the  $O^+$  losses hate, but a fell kilometer above ( $\sim 35$ km) with a maximum production rate of  $\sim 88 \cdot 10^{-3} [H^+].kp^{-1}$  also at 04:00 LT while the production peak of  $He^+$  suffers a little variation with time passing from 899 to 862 km of altitude with values of  $\sim 2 \cdot 10^{-3}$  and  $\sim 15 \cdot 10^{-3} [He^+].kp^{-1}$  at 00:30 and 4:00 LT, respectively.

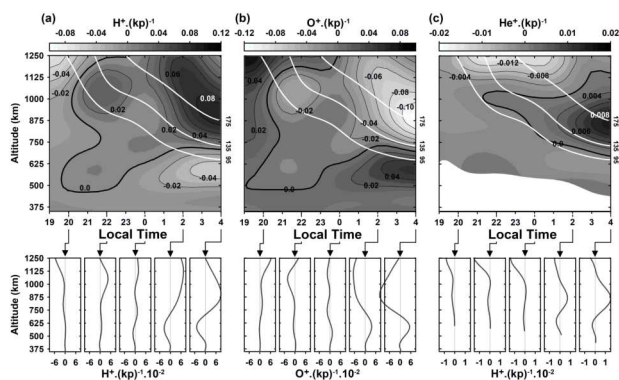


**Figure 3.** Ion fraction rates dependent of  $kp$  index. Top panels are showing the ions fraction rates contour plots by local time and altitude with intervals of 0.015 ( $H^+$  and  $O^+$ ) and 0.0017 ( $He^+$ )  $[I].(kp)^{-1}$ . The bottom panels are showing the vertical cuts of the same parameters for five different hours.

### 4 Conclusions

We presented analyzes of six nighttime's incoherent radar data from the June solstice separated by almost two years. We focused our analyzes on the dependence of the main ions in the topside ionosphere and the transition height of the ions  $H^+$  and  $O^+$  with the variations of the dissymmetric solar flux and  $kp$  indexes. The main results are listed below:

- The results have shown a loss layer of the  $He^+$  dependent of solar flux proportional to the difference between the ion fraction rates of the  $O^+$  and  $H^+$ ;
- By the  $He^+$  ion fraction rates it was possible to detect a strong dependence of this concentration with the solar

flux in altitudes above  $\sim 900$ km after midnight local time, and;

- The major variations of all the ion fraction rates with the geomagnetic activity were detected soon after midnight local time. At the same local time, a layer formed of the  $He^+$  with the increase of the geomagnetic activity was detected.

### 5 Acknowledgements

Arecibo Observatory is operated by the University of Central Florida under a cooperative agreement with the National Science Foundation (AST-1744119) and in alliance with Yang Enterprises and Ana G. Méndez-Universidad Metropolitana. The  $Kp$  index was obtained from the World Data Center for Geomagnetism, Kyoto (<http://wdc.kugi.kyoto-u.ac.jp/index.html>). A.M. Santos thanks the financial support from FAPESP (process number: 2015/25357-4). The

### 6 References

- Brum, C. G. M., Rodrigues, F. S., dos Santos, P. T., Matta, A. C., Aponte, N., Gonzalez, S. A., and Robles, E. (2011), A modeling study of  $f_oF_2$  and  $h_mF_2$  parameters measured by the Arecibo incoherent scatter radar and comparison with IRI model predictions for solar cycles 21, 22, and 23, *J. Geophys. Res.*, 116, A03324, doi:10.1029/2010JA015727
- Garzón, D. P., C. G. M. Brum, E. Echer, N. Aponte, M. P. Sulzer, S. A. González, R. B. Kerr, and Waldrop, L. (2011), Response of the topside ionosphere over Arecibo to a moderate geomagnetic storm. *J. Atmos. Sol. Terr. Phys.*, 73, 1568– 1574. doi:10.1016/j.jastp.2011.02.016
- Goncharenko, L. P., Hsu, V. W., Brum, C. G. M., Zhang, S.-R., and Fentzke, J. T. (2013), Wave signatures in the midlatitude ionosphere during a sudden stratospheric warming of January 2010, *J. Geophys. Res. Space Physics*, 118, 472– 487, doi:10.1029/2012JA018251
- Gonzalez, S.A. Radar, satellite, and modeling studies of the low latitude protonosphere. PhD Thesis, Utah State University, Logan, Utah, 1994. doi:10.13140/RG.2.1.1195.3369
- MacPherson, B., Models of the thermal plasma behaviour in the terrestrial ionosphere: Transport equations and Arecibo observations, Ph.D. thesis, Univ. of Sheffield, Sheffield, U.K., 1997.
- Wrenn, G., Rodger, A. S., & Rishbeth, H. (1987). Geomagnetic storms in the Antarctic  $F$ -region. I. Diurnal and seasonal patterns for main phase effects. *Journal of Atmospheric and Solar-Terrestrial Physics*, 49(9), 901– 913. doi:10.1016/0021-9169(87)90004-3